



CrossMark  
click for updates

# An efficient Fe<sub>2</sub>O<sub>3</sub>/HY catalyst for Friedel–Crafts acylation of *m*-xylene with benzoyl chloride

Manman Mu,<sup>ab</sup> Ligong Chen,<sup>ab</sup> Yunlong Liu,<sup>a</sup> Wangwang Fang<sup>a</sup> and Yang Li<sup>\*ab</sup>

Cite this: *RSC Adv.*, 2014, 4, 36951

Received 27th May 2014  
Accepted 10th July 2014

DOI: 10.1039/c4ra04984e

www.rsc.org/advances

Iron oxide supported on HY zeolite was prepared and exhibited excellent catalytic performance in the acylation of *m*-xylene with benzoyl chloride. It was characterized by XRD, BET, XPS, NH<sub>3</sub>-TPD and Py-IR. The obtained results indicated that the catalytic activity of Fe<sub>2</sub>O<sub>3</sub>/HY is enhanced with the increase of Lewis acidic sites. Furthermore, the reaction parameters, including load of Fe<sub>2</sub>O<sub>3</sub>, temperature, molar ratio and the dose of catalyst, were optimized. Thus the acylation proceeds effectively to afford 2,4-dimethylphenylacetophenone in 94.1% yield under optimum conditions. Finally, the catalyst was examined for the acylations of a series of arenes, all of the alkyl substituted benzenes were transformed to the corresponding products in satisfactory yields while the acylation of chlorobenzene was sluggish. The catalyst was easily separated from the reaction mixture and reused for five runs without appreciable loss of catalytic activity.

## 1. Introduction

Friedel–Crafts acylation of arenes is considered as an important method for the production of aromatic ketones, which are the key intermediates or final products in the pharmaceutical, agrochemical and cosmetic industries.<sup>1–3</sup> Traditionally, Lewis acids (such as AlCl<sub>3</sub>, FeCl<sub>3</sub>, TiCl<sub>4</sub> and BF<sub>3</sub>) or strong Brønsted acids (such as concentrated H<sub>2</sub>SO<sub>4</sub>) are required as the vital catalysts for this reaction. However, these catalysts normally suffer from highly toxic, corrosive, and discarding a large amount of waste water.<sup>4</sup> Recently, zeolite,<sup>5,6</sup> clay,<sup>7</sup> Nafion-H,<sup>8</sup> sulfated zirconia<sup>9</sup> and Keggin-type heteropolyacid<sup>10</sup> as solid acid catalysts are widely used in Friedel–Crafts acylations.

Nowadays, metal oxide especially iron oxide as catalysts have been widely used for various reaction, such as oxidation<sup>11</sup> and hydrogenation,<sup>12,13</sup> but little research was reported on the Friedel–Crafts acylation. Moreover, zeolites, well-known

microcrystalline porous materials, exhibit Lewis and Brønsted acidity, thermal stability, shape selectivity and ease to separation. Chiche and co-workers firstly reported the acylation of toluene with aliphatic acids over CeNaY zeolite. This catalyst showed an extraordinary high *para* shape-selectivity. However, the reactions required severe reaction conditions and gave poor yields.<sup>14</sup> Recently, V. N. Sheemol<sup>15</sup> reported that the catalytic activity can be improved by the modification of H-Beta zeolite with simple cation exchange (La<sup>3+</sup>, Ce<sup>3+</sup>, Dy<sup>3+</sup>). Moreover, Laidlaw and co-workers<sup>16</sup> claimed that Zn- and Fe-exchanged zeolites (HZSM-5, HY and mordenite) for toluene benzylation are more effective than the original zeolites. They also discovered that Fe-exchanged zeolites gave limited leaching of Fe cations into solution compared to other metal cations. Nowadays, catalyst deactivation was the main hindrance in the large-scale industrial applications of modified zeolite catalysts.<sup>17</sup>

Thus, in the present work, several metal oxides supported on HY zeolite were examined for the acylation of *m*-xylene with benzoyl chloride (Scheme 1), and the best catalytic performance was displayed by Fe<sub>2</sub>O<sub>3</sub>/HY. These catalysts were comparatively characterized by Brunauer–Emmett–Teller (BET), X-ray diffraction (XRD), X-ray Photoelectron Spectroscopy (XPS), NH<sub>3</sub>-temperature programmed desorption (TPD) and IR spectra of adsorbed pyridine (Py-IR). The influence of the Si/Al ratio (SAR) of the support was evaluated. Additionally, the reaction parameters such as load of Fe<sub>2</sub>O<sub>3</sub>, temperature, molar ratio of the reactants and the dose of catalyst were also optimized.

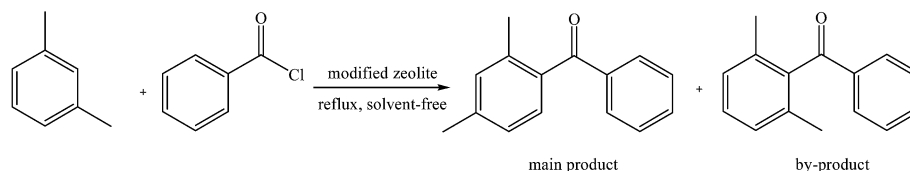
## 2. Experimental

### 2.1 Materials and catalysts

The zeolites, HY (Si/Al = 7, 9, 11), HBeta (Si/Al = 25), ZSM-5 (Si/Al = 25) and mordenite, were purchased from Nankai University Catalyst Co., Tianjin, China. *m*-Xylene (AR) and benzoyl chloride (AR) were obtained from Tianjin Guangfu Fine-chemical institute, Tianjin, China. Commercially available reagents were used without further purification.

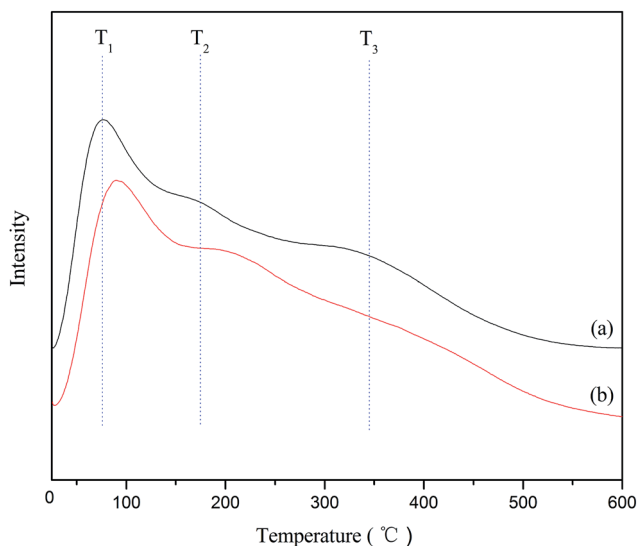
<sup>a</sup>School of Chemical Engineering and Technology, Tianjin University, Tianjin 300072, China. E-mail: liyang777@tju.edu.cn; Fax: +86-22-27406314; Tel: +86-22-27406314

<sup>b</sup>Collaborative Innovation Center of Chemical Science and Engineering, Tianjin 300072, China

Scheme 1 Acylation of *m*-xylene with benzoyl chloride.Table 1 Catalytic performance of catalysts in the acylation of *m*-xylene with benzoyl chloride<sup>a</sup>

Entry	Catalyst	Conversion <sup>b</sup> (%)	Selectivity <sup>c</sup> (%)	Yield (%)
1	HY	30.37	82.52	25.06
2	Mordenite	27.06	73.59	19.91
3	HZSM-5	23.50	68.42	16.08
4	HBeta	16.49	81.29	13.40
5	Fe <sub>2</sub> O <sub>3</sub> /HY	97.29	93.74	91.20
6	NiO/HY	89.95	91.70	82.48
7	CoO/HY	72.56	94.69	68.71
8	Al <sub>2</sub> O <sub>3</sub> /HY	37.55	80.04	30.06
9	CeO/HY	—	—	—
10	LaO/HY	—	—	—

<sup>a</sup> Reaction condition: *m*-xylene : benzoyl chloride = 4 : 1; the amount of catalyst = 5 wt%; *T* = 130 °C. <sup>b</sup> The conversion of benzoyl chloride. <sup>c</sup> The selectivity of 2,4-dimethylphenyl-acetophenone.

Fig. 1 NH<sub>3</sub>-TPD curves for (a) HY, (b) Fe<sub>2</sub>O<sub>3</sub>/HY.

The catalysts used in this study were prepared by the equal-volume impregnation method. For example, Fe<sub>2</sub>O<sub>3</sub>/HY was prepared as follows. HY zeolites (10 g) were impregnated with

10.0 mL aqueous solution of 1.5 g iron nitrate hexahydrate (15 wt%). After impregnating at ambient temperature for 4 h, it was dried at 110 °C for 5 h and calcined at 550 °C for 5 h. Several metal oxides (CoO, NiO, LaO, CeO and Al<sub>2</sub>O<sub>3</sub>) supported on HY zeolite were prepared by the same method. Furthermore, Fe<sub>2</sub>O<sub>3</sub>/HY catalysts with different Fe<sub>2</sub>O<sub>3</sub> loads were also prepared and hereinafter referred to as xFe<sub>2</sub>O<sub>3</sub>/HY (*x* = 10–20%).

## 2.2 Characterization

The crystallinity of catalysts was determined by X-ray powder diffraction with Rigaku D/max 2500 X-ray diffractometer using Cu-K $\alpha$  radiation (40 kV, 100 mA) in the range of 5–90 °C. The specific surface areas were determined by the BET method with N<sub>2</sub> adsorption-desorption measurements at liquid nitrogen temperature using a NOVA 2000e analyzer. IR spectra were obtained using the KBr method on a Nicolet system. X-ray photoelectron spectroscopy (XPS) was recorded on a PHI1600 spectrometer with a Mg K $\alpha$  X-ray source for excitation. NH<sub>3</sub>-TPD was conducted with a ChemiSorb 2750 instrument at an

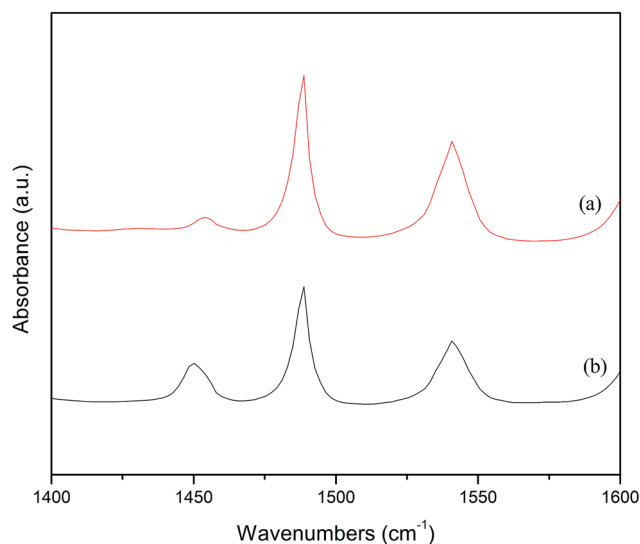
Fig. 2 Py-IR spectra of (a) HY and (b) Fe<sub>2</sub>O<sub>3</sub>/HY.

Table 2 Acid capacity of two catalysts

Catalysts	Low temperature peak area [a. u.]	Medium temperature peak area [a. u.]	High temperature peak area [a. u.]	Total peak area [a. u.]
HY	2.2690	3.6477	6.9408	12.8575
Fe <sub>2</sub> O <sub>3</sub> /HY	2.7915	4.5259	5.8038	13.1212

**Table 3** Integrated areas for Brønsted and Lewis acid sites in FT-IR spectra of adsorbed pyridine on HY and Fe<sub>2</sub>O<sub>3</sub>/HY catalysts

Catalysts	Integrated areas <sup>a</sup>		L/(B + L) ratio
	Brønsted	Lewis	
HY	46.03	23.99	0.34
Fe <sub>2</sub> O <sub>3</sub> /HY	42.91	29.88	0.41

<sup>a</sup> Integrated areas of Lewis and Brønsted acid sites were based on band at 1450 cm<sup>-1</sup> and 1540 cm<sup>-1</sup>, respectively.

atmospheric pressure with a thermal conductivity detector device. The IR spectra of adsorbed pyridine were recorded on a Thermo Nicolet Nexus 470 spectrometer equipped with a heatable and evacuable IR cell containing CaF<sub>2</sub> windows.

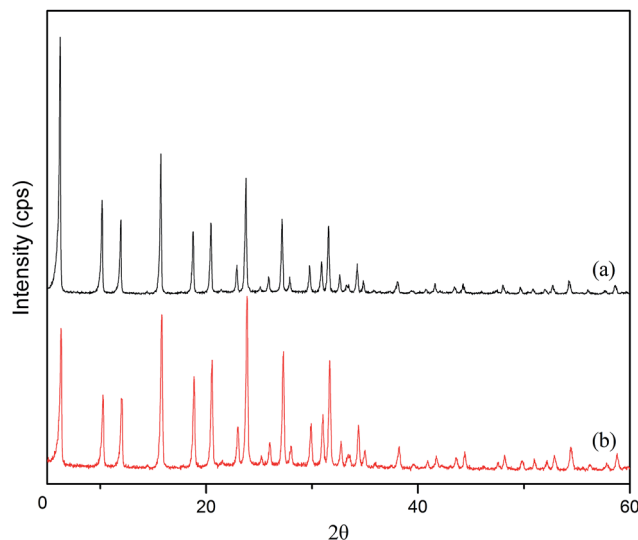
### 2.3 General procedures for the acylation of *m*-xylene with benzoyl chloride

A mixture of *m*-xylene (40 mmol), benzoyl chloride (10 mmol) and catalyst (70 mg, 5 wt%) was magnetically stirred and heated to reflux (130 °C) for 5 h. The catalyst was separated from the reaction mixture by simple filtration and then the filtrate was analyzed by gas chromatography (SE-30 capillary column: 60 m × 0.25 mm, 0.2 μm film thickness) and the composition of the reaction mixture was confirmed by GC-MS (HP-1 capillary column: 30 m × 0.25 mm, 0.2 μm film thickness).

## 3. Results and discussion

### 3.1 Catalyst selection

As mentioned above, solid acids were intensively studied for the alkylation and acylation of arenes recently. Thus, several zeolites, including HY, HBeta, ZSM-5 and mordenite were firstly selected as catalysts for the acylation of *m*-xylene with benzoyl chloride in this study. The obtained results were summarized in Table 1 (entry 1–4). It was obvious that these zeolite catalysts presented low activity, the conversion of *m*-xylene were all less than 30.0%. This is possibly attributed to the weak Lewis acidity of zeolites. Therefore, in order to enhance the Lewis acidity of catalysts, several metal oxides were doped into HY zeolite, the obtained catalysts were examined for the above reaction, and the results were presented in Table 1 (entry 5–10). The experimental results showed that Fe<sub>2</sub>O<sub>3</sub>/HY catalyst displayed much better catalytic performance than the other catalysts, the conversion of *m*-xylene was 97.3%. Therefore, Fe<sub>2</sub>O<sub>3</sub>/HY was chosen as the catalyst for the following study. To further

**Fig. 3** XRD patterns of (a) HY and (b) Fe<sub>2</sub>O<sub>3</sub>/HY.

understand these results, these catalysts were studied by NH<sub>3</sub>-TPD, Py-IR and XRD.

### 3.2 Characterization

**3.2.1 NH<sub>3</sub>-TPD and Py-IR.** In this study, extensive NH<sub>3</sub>-TPD studies were performed to compare the acidity distinction between HY and Fe<sub>2</sub>O<sub>3</sub>/HY and the TPD curves were shown in Fig. 1. Both of them exhibited three typical desorption peaks, which could be assigned to the weak (50–150 °C, T<sub>1</sub>), medium (150–300 °C, T<sub>2</sub>) and strong acid sites (300–600 °C, T<sub>3</sub>), respectively. It was obvious that the desorption temperature on the weak acid sites increased with iron oxide introduction. Therefore, the strength of the weak acid sites on Fe<sub>2</sub>O<sub>3</sub>/HY was apparently higher than that of HY catalyst. Furthermore, the area of a specific peak could be used to estimate the amount of ammonia desorbed from the sample and taken as a standard to quantify the acid capacity of the sample.<sup>18</sup> As summarized in Table 2, the total acid capacity of Fe<sub>2</sub>O<sub>3</sub>/HY is a little higher than that of HY catalyst while its strong acid capacity is less than HY.

To get further information about the Brønsted and Lewis acid sites, Py-IR spectra of HY and Fe<sub>2</sub>O<sub>3</sub>/HY were performed (Fig. 2). The bands at 1540 cm<sup>-1</sup> and 1450 cm<sup>-1</sup> were attributed to the pyridine adsorbed on the Brønsted and Lewis acid sites, respectively.<sup>19</sup> The integrated areas for Brønsted and Lewis acid sites were obtained and the calculated L/(L + B) ratios were listed in Table 3. The results demonstrated that both the

**Table 4** Textural properties of the catalysts

Samples	Surface area (m <sup>2</sup> g <sup>-1</sup> )		Pore volume <sup>b</sup> (cm <sup>3</sup> g <sup>-1</sup> )	Average pore diameter <sup>a</sup> (Å)
	Total	Micropore <sup>a</sup>		
HY	663.2	619.1	0.36	1.09
Fe <sub>2</sub> O <sub>3</sub> /HY	649.9	585.9	0.37	1.14

<sup>a</sup> Calculated by the *t*-plot method. <sup>b</sup> Calculated by the Barrett–Joyner–Halenda (BJH) method.

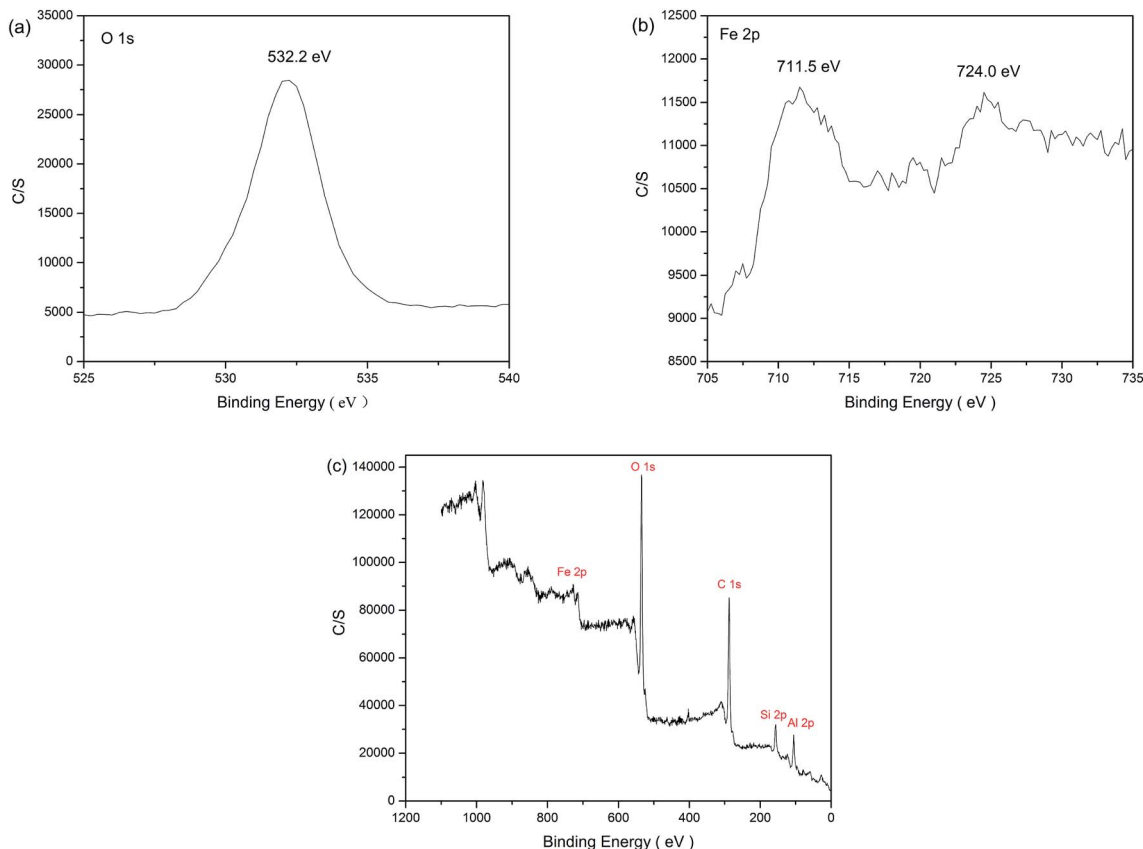


Fig. 4 XPS spectra of  $\text{Fe}_2\text{O}_3/\text{HY}$  catalyst.

amounts of Lewis acid sites and  $L/(L + B)$  ratio increase remarkably by doping  $\text{Fe}_2\text{O}_3$  into HY zeolite. This result obviously revealed that Lewis acid sites are more important than Brönsted acid sites for the acylation of *m*-xylene with benzoyl

chloride. This is the possible reason that  $\text{Fe}_2\text{O}_3/\text{HY}$  exhibited excellent catalytic activity. Based on the analysis from Fig. 2 and Table 3, we could conclude that the conversion of *m*-xylene was improved with the increase of Lewis acid sites.

**3.2.2 Textural properties of catalysts.** The specific surface areas and pore structural parameters of HY and  $\text{Fe}_2\text{O}_3/\text{HY}$  are summarized in Table 4. In comparison with HY zeolite, the total and micropore surface area of  $\text{Fe}_2\text{O}_3/\text{HY}$  decreased a little. Meanwhile, there was no significant change for the pore size. It was obvious that the morphology structure of HY was almost unchanged by doping  $\text{Fe}_2\text{O}_3$  into HY catalyst. Nevertheless,  $\text{Fe}_2\text{O}_3/\text{HY}$  exhibited better catalytic activity than HY zeolite (see Table 1), this indicated that iron oxide in  $\text{Fe}_2\text{O}_3/\text{HY}$  play an important role as the active species in the acylation of *m*-xylene with benzoyl chloride.

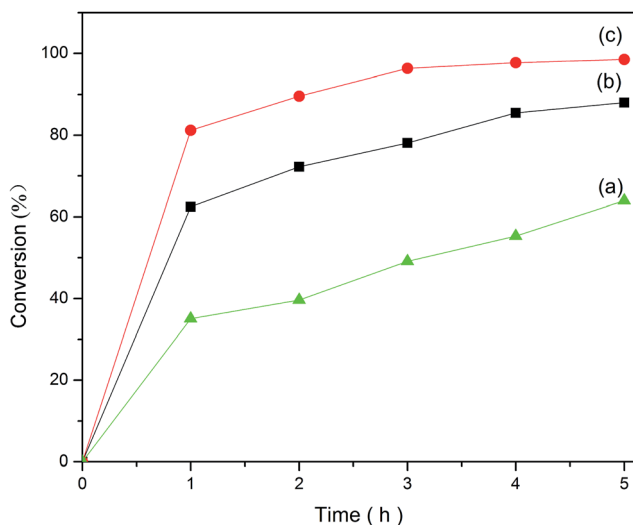


Fig. 5 Influence of  $\text{Fe}_2\text{O}_3$  load on the conversion of benzoyl chloride. *m*-xylene : benzoyl chloride = 4 : 1; catalyst dose = 5 wt%;  $T = 110^\circ\text{C}$ . (a) 10 wt%, (b) 15 wt%, (c) 20 wt%.

Table 5 Effect of Si/Al ratio of HY zeolite to the reaction<sup>a</sup>

Entry	Catalyst	Conversion (%)	Selectivity (%)	Yield (%)
1	$\text{Fe}_2\text{O}_3/\text{HY}(\text{Si}/\text{Al} = 7)$	99.58	94.48	93.88
2	$\text{Fe}_2\text{O}_3/\text{HY}(\text{Si}/\text{Al} = 9)$	80.63	95.31	76.85
3	$\text{Fe}_2\text{O}_3/\text{HY}(\text{Si}/\text{Al} = 11)$	79.39	89.12	70.75

<sup>a</sup> Reaction condition: *m*-xylene : benzoyl chloride = 4 : 1; catalyst dose = 5 wt%;  $T = 130^\circ\text{C}$ .

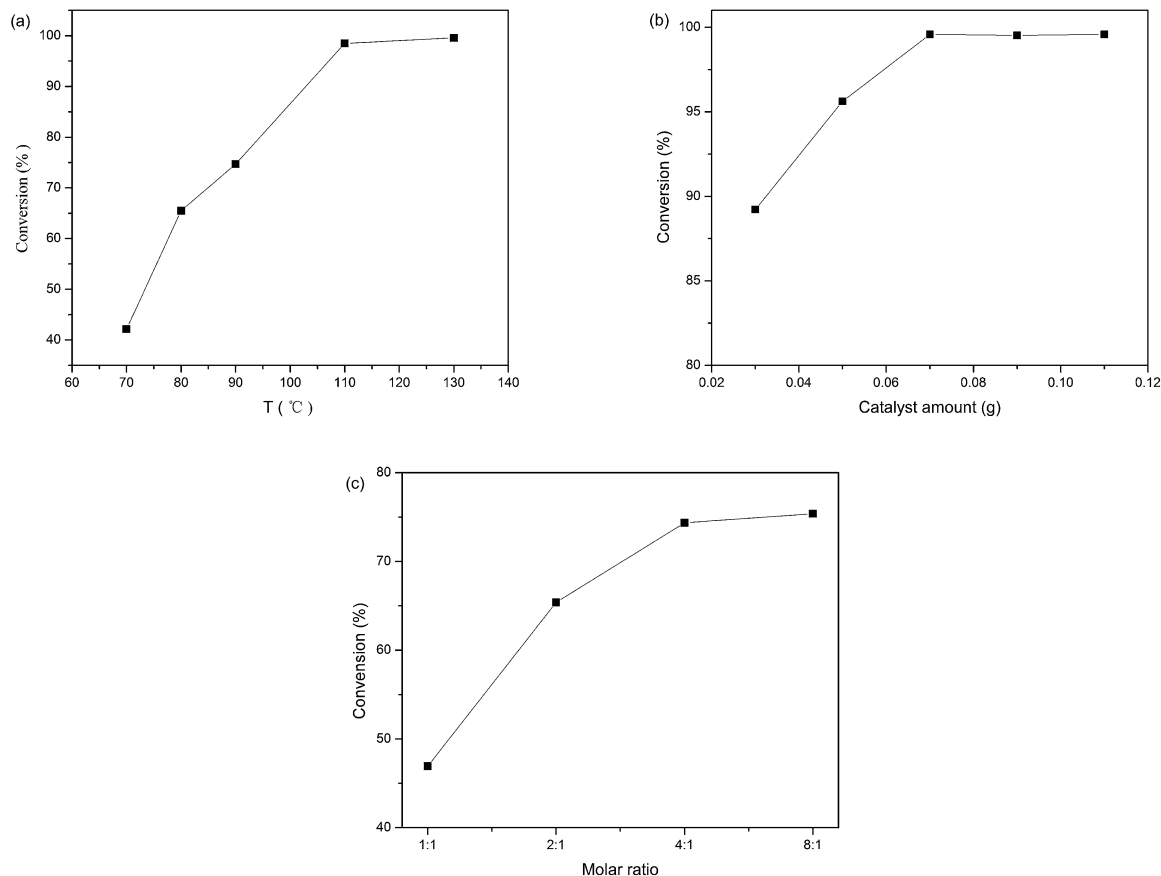


Fig. 6 (a) Influence of reaction temperature on the conversion of benzoyl chloride *m*-xylene : benzoyl chloride = 4 : 1; catalyst dose = 5 wt%. (b). Influence of catalyst amount on the conversion of benzoyl chloride. *m*-xylene : benzoyl chloride = 4 : 1;  $T = 130$  °C. (c) Influence of molar ratio of *m*-xylene/benzoyl chloride on the conversion of benzoyl chloride. catalyst dose = 5 wt%;  $T = 90$  °C.

**3.2.3 XRD.** The XRD patterns of HY and  $\text{Fe}_2\text{O}_3/\text{HY}$  were shown in Fig. 3. All samples exhibited the typical diffraction peaks of the faujasite (FAU) structure. However, the intensity of the peaks for  $\text{Fe}_2\text{O}_3/\text{HY}$  decreased slightly. It was probably due to the change in the crystallinity when  $\text{Fe}_2\text{O}_3$  was distributed on the HY surface.<sup>20,21</sup> Furthermore, the diffraction spectra of  $\text{Fe}_2\text{O}_3$  could not be observed on the XRD patterns of  $\text{Fe}_2\text{O}_3/\text{HY}$  catalyst. The results suggested that  $\text{Fe}_2\text{O}_3$  species were either in the amorphous form or highly dispersed as very small particles on HY zeolite. Similar phenomena were reported for  $\text{TiO}_2$  supported on HY and iron supported on mesoporous silica.<sup>22,23</sup>

**3.2.4 XPS.** The XPS spectra of  $\text{Fe}_2\text{O}_3/\text{HY}$  catalyst was presented in Fig. 4. The typical Fe 2p XPS narrow scan spectrum presented two main peaks at about 711.5 and 724.0 eV corresponding to the spin-orbit split doublet of Fe 2p<sub>3/2</sub> and Fe 2p<sub>1/2</sub> (Fig. 4b), which implied that the iron element on the catalyst surface existed mainly in the form of  $\text{Fe}^{3+}$  species. The O 1s XPS of the sample showed a single peak at 532.2 eV corresponding to the oxide oxygen ( $\text{O}^{2-}$ ) in  $\text{Fe}_2\text{O}_3$  (Fig. 4a). Therefore, these results indicated that the Fe species were predominantly in the form of  $\text{Fe}_2\text{O}_3$ .

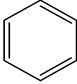
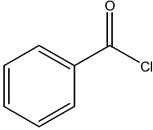
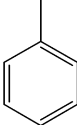
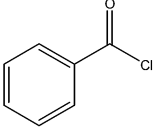
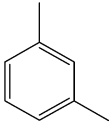
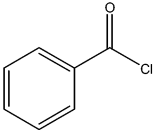
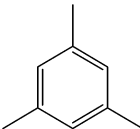
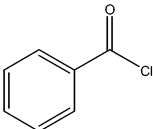
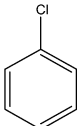
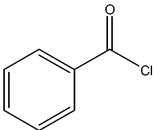
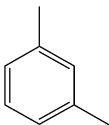
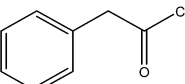
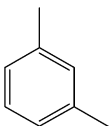
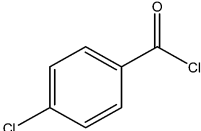
### 3.3 The effect of $\text{Fe}_2\text{O}_3$ load in $\text{Fe}_2\text{O}_3/\text{HY}$

The effect of  $\text{Fe}_2\text{O}_3$  load on the acylation of *m*-xylene with benzoyl chloride was investigated and the results were described in Fig. 5. With the increase of  $\text{Fe}_2\text{O}_3$  load from 10 to 15 wt%, the conversion of benzoyl chloride increased rapidly. According to the above discussion, with the increase of  $\text{Fe}_2\text{O}_3$  load, Lewis acidic sites increase, led to enhance the activity of  $\text{Fe}_2\text{O}_3/\text{HY}$ . However, when the load reached to 20 wt%, the conversion of benzoyl chloride displayed a slight drop as compared to 15 wt% load at the same reaction conditions. Thus 15 $\text{Fe}_2\text{O}_3/\text{HY}$  was selected for the acylation of *m*-xylene with benzoyl chloride.

### 3.4 The effect of Si/Al ratio of HY zeolite

Some researchers reported that the catalytic activity of zeolites on Friedel-Crafts acylation was influenced by the Si/Al ratio (SAR) of zeolite.<sup>24</sup> Thus, the effect of the SAR of HY support on the acylation of *m*-xylene with benzoyl chloride was examined and the results are listed in Table 5. It was obvious that the conversion of benzoyl chloride increased from 79.39% to 99.58% when the framework SAR value of HY zeolite decreased from 11 to 7. This was mainly due to the increase of the total

Table 6 Influence of various substrates or acylation reagents on acylation reaction

Entry	Substrate	Acylation reagent	Time (h)	Temperature (°C)	Conversion (%)	Yield (%)
1			5	80	14.58	6.33
2			10	110	66.68	43.20
3			5	130	99.58	93.39
4			3	110	100	100
5			10	130	—	—
6			5	130	95.39	74.74
7			5	130	91.48	87.49

Lewis acid sites with decrease of the SAR value of HY support, and then the increase of the catalytic activity was observed.

### 3.5 The effect of reaction parameters

The acylation of *m*-xylene with benzoyl chloride over Fe<sub>2</sub>O<sub>3</sub>/HY was examined at a temperature range from 70 to 130 °C and the results are shown in Fig. 6a. As the temperature increased, the conversion of benzoyl chloride increased sharply during 70–110 °C and then increased slightly above 110 °C. Thus, reflux temperature (130 °C) was chosen as the optimum reaction temperature.

The influence of the amount of catalyst on the conversion of benzoyl chloride was investigated ranged from 2 wt% to 8 wt%. It was found that the conversion of benzoyl chloride increased from 89.2% to 99.6% with an increase of the amount of catalyst from 2 to 5 wt% (Fig. 6b). Further increase to 8 wt%, no

appreciable effect was observed on the conversion of benzoyl chloride. Thus, 5 wt% was selected to be the suitable catalyst amount.

The effect of molar ratio of *m*-xylene and benzoyl chloride to the acylation was studied over Fe<sub>2</sub>O<sub>3</sub>/HY catalyst and the results were described in Fig. 6c. At a molar ratio of 1, the conversion of benzoyl chloride was only 47.1%. With the increase of the molar ratio from 1 to 4, the conversion of benzoyl chloride remarkably increased because the excess of *m*-xylene would enhance the transformation of benzoyl chloride. Thus, the molar ratio of *m*-xylene to benzoyl chloride was selected as 4.

As mentioned above, Fe<sub>2</sub>O<sub>3</sub>/HY catalyst displayed excellent catalytic activity in the acylation of *m*-xylene with benzoyl chloride. Therefore, the study was extended to the Friedel–Crafts acylation reaction of benzoyl chloride with several aromatic compounds having different substituents, including benzene, toluene, *m*-xylene, mesitylene and chlorobenzene.

Reactions were carried out under the optimum reaction conditions and the results are summarized in Table 6 (entry 1–5). As expected, the benzylation of mesitylene proceeded more effectively than *m*-xylene due to the presence of more electron donating groups. This result was quite consistent with the conventional Friedel–Crafts acylation reactions.<sup>1</sup> However, chlorobenzene was sluggish in the acylation and the conversion was low since the electron withdrawing nature of chloro group. Furthermore, Fe<sub>2</sub>O<sub>3</sub>/HY was employed in the acylations of *m*-xylene with phenylacetyl chloride and 4-chlorobenzoyl chloride, respectively (Table 6, entry 6, 7). It was found that the conversion of benzoyl chloride was 99.5%, while that of 4-chlorobenzoyl chloride was 91.5% at the same reaction conditions. This was mainly due to the synergistic effect of electron withdrawing induction and donating conjugation of chloride atom. Moreover, the conversion of phenylacetyl chloride was slightly lower than that of benzoyl chloride. It was attributed to the difficulty of forming phenylacetyl cation.

### 3.6 Reusability of the catalyst

The separation and reusability of catalysts are quite important for acylations. So the recycling experiments were performed over Fe<sub>2</sub>O<sub>3</sub>/HY and the results are presented in Fig. 7. The catalyst was separated from the reaction mixture by simple filtration, washed with ethanol and reused after drying at 110 °C for 5 h. It was seen from Fig. 7 that the conversion of benzoyl chloride displayed a slight drop after the third run. The decrease of benzoyl chloride conversion was probably attributed to the unavoidable trace mechanical loss of catalyst during work-up procedures. These results indicated that Fe<sub>2</sub>O<sub>3</sub>/HY catalyst exhibited excellent stability, no significant deactivation of Fe<sub>2</sub>O<sub>3</sub>/HY catalyst was detected during its reuse in the acylation.

Moreover, the acylation of *m*-xylene with benzoyl chloride over Fe<sub>2</sub>O<sub>3</sub> would be a homogeneously catalysed reaction. It

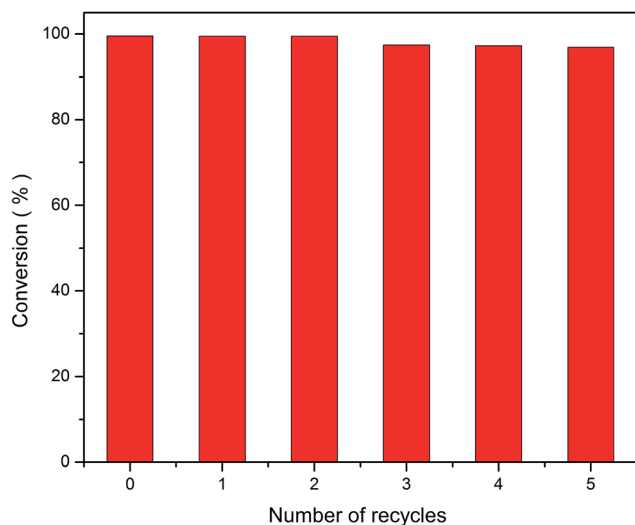


Fig. 7 Reusability of Fe<sub>2</sub>O<sub>3</sub>/HY catalyst. *m*-xylene : benzoyl chloride = 4 : 1; catalyst dose = 5 wt%; *T* = 130 °C.

would result in the formation of the soluble compound FeCl<sub>3</sub>, which was powerful homogeneous Friedel–Crafts catalyst. However, the obtained result indicated that the Friedel–Crafts acylation over Fe<sub>2</sub>O<sub>3</sub>/HY would be a well heterogeneously catalysed reaction. It could be due to the strong interaction of Fe<sub>2</sub>O<sub>3</sub> with HY zeolite, which inhibited the reaction of Fe<sub>2</sub>O<sub>3</sub> with benzoyl chloride.

## 4. Conclusions

In summary, iron oxide supported on HY zeolite was found to be an efficient, stable and reusable solid acid catalyst for Friedel–Crafts acylation reaction and exhibited excellent catalytic performance in the acylation of *m*-xylene with benzoyl chloride. 99.5% conversion of benzoyl chloride and 94.5% selectivity of 2,4-dimethylphenyl-acetophenone were achieved. The catalysts were characterized by XRD, BET, XPS, NH<sub>3</sub>-TPD, Py-IR and the results revealed that the catalytic activity of Fe<sub>2</sub>O<sub>3</sub>/HY was enhanced by the increase of Lewis acidic sites. Furthermore, it was found that the catalytic activity increased with the SAR decrease of HY zeolite. The influences of iron oxide load, temperature, molar ratio and catalyst dose were investigated and optimized. The reusability tests of the catalyst showed that this catalyst can be used five runs without appreciable loss in catalytic activity.

## References

- 1 P. H. Gore, in *Aromatic Ketone Synthesis in Friedel–Crafts and Related Reactions*, ed. G. A. Olah, John Wiley & Sons Inc., London, 1964, vol. III, part 1, p. 1.
- 2 H. G. Franck, J. W. Stadelhofer, *Industrial Aromatic Chemistry*, Springer, Berlin, 1988.
- 3 S. Gmouh, H. Yang and M. Vaultier, *Org. Lett.*, 2003, **5**, 2219–2222.
- 4 J. Ross and J. Xiao, *Green Chem.*, 2002, **4**, 129–133.
- 5 D. Das and S. Cheng, *Appl. Catal., A*, 2000, **201**, 159–168.
- 6 M. Bejblová, D. Procházková and J. Čejka, *ChemSusChem*, 2009, **2**, 486–499.
- 7 J. Farkas, S. Békássy and B. Ágai, *Synth. Commun.*, 2000, **30**, 2479–2485.
- 8 T. Yamato, C. Hideshima and G. K. Surya Prakash, *J. Org. Chem.*, 1991, **56**, 2089–2091.
- 9 K. Arata, H. Nakamura and M. Shouji, *Appl. Catal., A*, 2000, **197**, 213–219.
- 10 T. Okuhara, N. Mizuno and M. Misono, *Adv. Catal.*, 1996, **41**, 113–252.
- 11 M. B. Gawande, P. S. Branco and I. D. Nogueira, *Green Chem.*, 2013, **15**, 682–689.
- 12 R. V. Jagadeesh, A. E. Surkus and H. Junge, *Science*, 2013, **342**, 1073–1076.
- 13 M. B. Gawande, P. S. Branco and R. S. Varma, *Chem. Soc. Rev.*, 2013, **42**, 3371–3393.
- 14 B. Chiche, A. Finiels, C. Gauthier, P. Geneste, J. Graille and D. Pioch, *J. Org. Chem.*, 1986, **51**, 2128–2130.
- 15 V. N. Sheemol, B. Tyagi and R. V. Jasra, *J. Mol. Catal. A: Chem.*, 2004, **215**, 201–208.

- 16 P. Laidlaw, D. Bethella and S. M. Brown, *J. Mol. Catal. A: Chem.*, 2001, **174**, 187–191.
- 17 D. Rohan, C. Canaff, P. Magnoux and M. Guisnet, *J. Mol. Catal. A: Chem.*, 1998, **129**, 69–78.
- 18 D. Ma, W. P. Zhang, Y. Y. Shu, X. M. Liu, Y. D. Xu and X. H. Bao, *Catal. Lett.*, 2000, **66**, 155–160.
- 19 K. Rhee, U. Rao, J. Stencel, G. Melson and J. Crawford, *Zeolites*, 1983, **3**, 337–347.
- 20 N. F. Jaafar, A. A. Jalil and S. Triwahyono, *Chem. Eng. J.*, 2012, **191**, 112–122.
- 21 N. An, Q. Yu, G. Liu, S. Li, M. Jia and W. Zhang, *J. Hazard. Mater.*, 2011, **186**, 1392–1397.
- 22 H. Chen, A. Matsumoto, N. Nishimiya and K. Tsutsumi, *Colloids Surf., A*, 1999, **157**, 295–305.
- 23 X. Wang, Q. Zhang, S. Yang and Y. Wang, *J. Phys. Chem. B*, 2005, **109**, 23500–23508.
- 24 P. Botella, A. Corma, J. M. López-Nieto, S. Valencia and R. Jacquot, *J. Catal.*, 2000, **195**, 161–168.